

# Supplementary Materials

## Highly efficient heterogeneous Pd@POPs catalyst for the N-formylation of amine and CO<sub>2</sub>

Guoqing Wang,<sup>[a,b]</sup> Miao Jiang,<sup>[a]</sup> Guangjun Ji,<sup>[a,b]</sup> Zhao Sun,<sup>[a,b]</sup> Lei Ma,<sup>[a]</sup> Cunyao Li,<sup>[a]</sup> Hong Du,<sup>[a]</sup> Li Yan,<sup>\*,[a,b]</sup> Yunjie Ding<sup>\*,[a,b,c]</sup>

[a] Dalian National Laboratory for Clean Energy, Dalian Institute of Chemical Physics, Chinese Academy of Sciences, Dalian 116023, Liaoning, China

[b] University of Chinese Academy of Sciences, Beijing 100049, China

[c] State Key Laboratory of Catalysis, Dalian Institute of Chemical Physics, Chinese Academy of Sciences, Dalian 116023, Liaoning, China.

Correspond author: [yanli@dicp.ac.cn](mailto:yanli@dicp.ac.cn)

[dyj@dicp.ac.cn](mailto:dyj@dicp.ac.cn)

Number of Pages: 13

Number of Figures: 10

Number of Tables: 0

## Table of Contents

**Page S3:** The parameter of Characterization instrument.

**Page S5:** The TG curves (Figure S1).

**Page S6:** GC spectra of reaction solution of 1a (Figure S2).

**Page S6:** NMR spectrum of reaction solution of 2a (Figure S3).

**Page S7:** NMR spectrum of reaction solution of 3a (Figure S4).

**Page S8:** NMR spectrum of reaction solution of 4a (Figure S5).

**Page S9:** NMR spectrum of reaction solution of 5a (Figure S6).

**Page S10:** NMR spectrum of reaction solution of 6a (Figure S7).

**Page S11:** NMR spectrum of reaction solution of 7a (Figure S8).

**Page S12:** NMR spectrum of reaction solution of 8a (Figure S9).

**Page S13:** NMR spectrum of reaction solution of 9a (Figure S10).

## 1. Characterization of catalyst

N<sub>2</sub> adsorption isotherms were obtained by N<sub>2</sub> physisorptions measurements using a Quantachrome Autosorb-1 at 77 K. About 25 mg samples were employed for each test. The powder samples were outgassed for 10 h at 393 K before the measurements. The specific surface areas were calculated from the adsorption data using the Brunauer-Emmett-Teller (BET) method. The pore size distribution curves were obtained from the adsorption branches using the non-local density functional theory (NLDFT) method.

Transmission electron microscopy (TEM) images were obtained using a JEM-2100 with an accelerating voltage of 200 kV. The point resolution was 0.23 nm while the linear resolution was 0.14 nm. Scanning electron microscopy (SEM) was performed using a JSM-7800F with an accelerating voltage of 0.01-30 kV. The resolution of the secondary electron image was 0.8 nm at 15 kV and 1.2 nm at 1 kV while the resolution of the backscatter electron image was 1.5 nm at 15 kV.

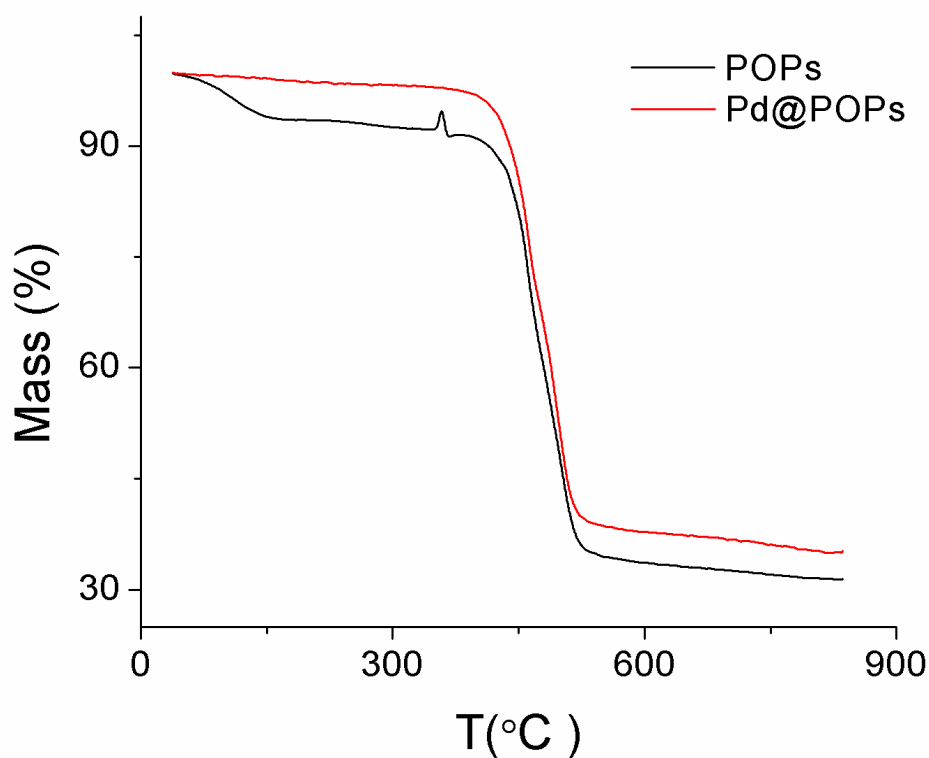
Thermogravimetric analysis (TGA) was carried out using a thermal analyzer (NETZSCH STA 449F3), the samples were heated at the rate of 10 K/min from room temperature up to 923 K in a flow of nitrogen. 6.95 mg of the powder sample was employed. The gas flow of the protective gas (N<sub>2</sub>) was fixed at 20 ml/min, and the gas flow of the carrier gas (N<sub>2</sub>) was also fixed at 20 ml/min.

Solid-state <sup>31</sup>P MAS NMR experiments were carried out on a Bruker Avance III spectrometer (9.4 T) equipped with 4 mm HXY probes in double resonance mode at a

frequency of 162 MHz. The experiments were carried out at a magic angle spinning rate of 13 kHz and a delay of 3 s. Solid-state  $^{31}\text{P}$  NMR chemical shifts were referenced to  $(\text{NH}_4)_2\text{HPO}_4$ . And  $^{13}\text{C}$  MAS NMR spectra were recorded at a magic angle spinning rate of 13 kHz and a delay of 1.5 s. Solid-state  $^{13}\text{C}$  NMR chemical shifts were referenced to CH of adamantane. About 35 mg of powder samples were filled in the  $\text{ZrO}_2$  sample cell when testing.

X-ray photoelectron spectroscopy spectrum were conducted using KRATOS, Axis Ultra<sup>DLD</sup> with the Al  $K\alpha$  irradiation ( $h\nu$  is 1486.6 eV) for X-ray sources, and the spectrometer binding energy was calibrated through the reference C 1s (284.6 eV). The pressure of the vacuum chamber was kept lower than  $9.8 \times 10^{-10}$  mbar when testing while a step size of 0.05/0.10 eV was employed.

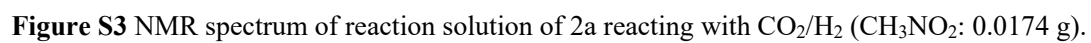
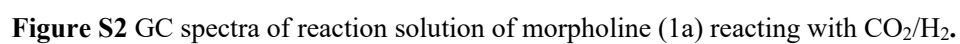
## 2. Supplementary Figure

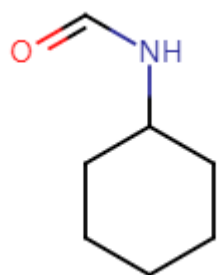


**Figure S1** TG curves of POPs (black) and Pd@POPs (red).

## 2. Determination of the product yields

The structure of 1a was characterized by comparing the retention time with the authentic compound and GC-MS. The yield was determined by GC using toluene as the internal standard. For 2b-9b, NMR yields were given. The  $^1\text{H}$  NMR ( $\text{CDCl}_3$ , 400 MHz) spectra of the reaction mixture and MS spectra of the product were shown below.





3b

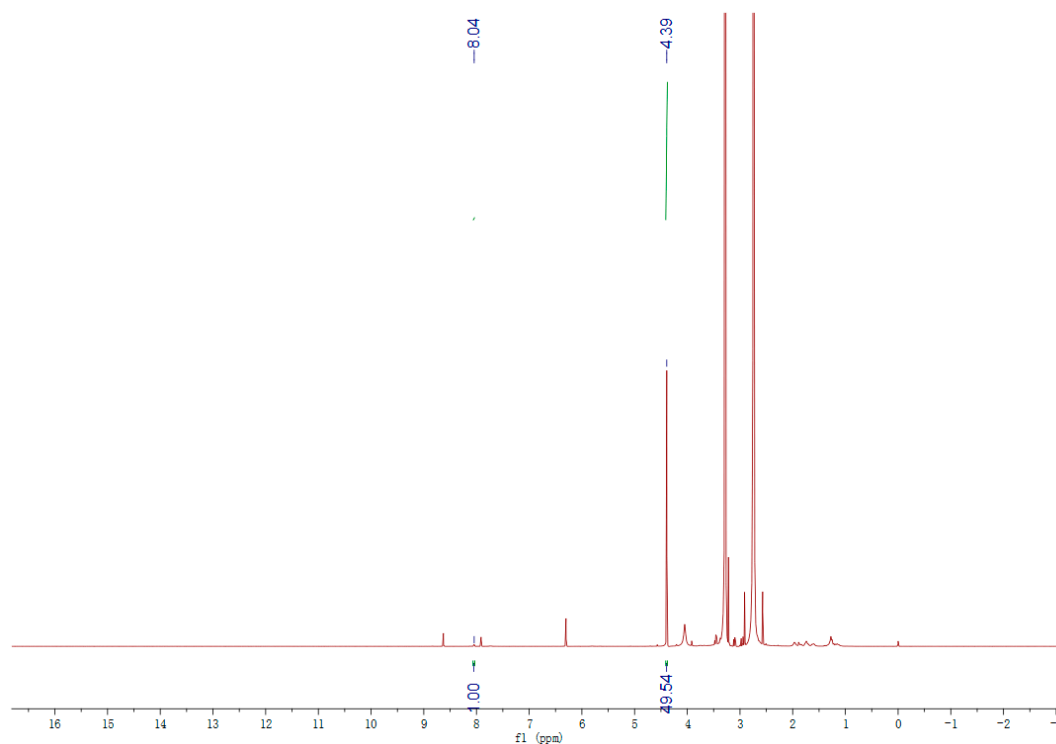
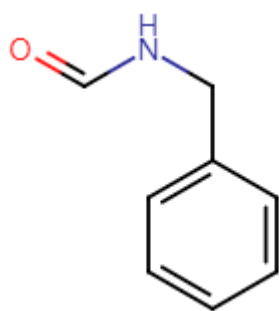


**Figure S4** NMR spectrum of reaction solution of 3a reacting with CO<sub>2</sub>/H<sub>2</sub> (CH<sub>3</sub>NO<sub>2</sub>: 0.0184 g).



4b

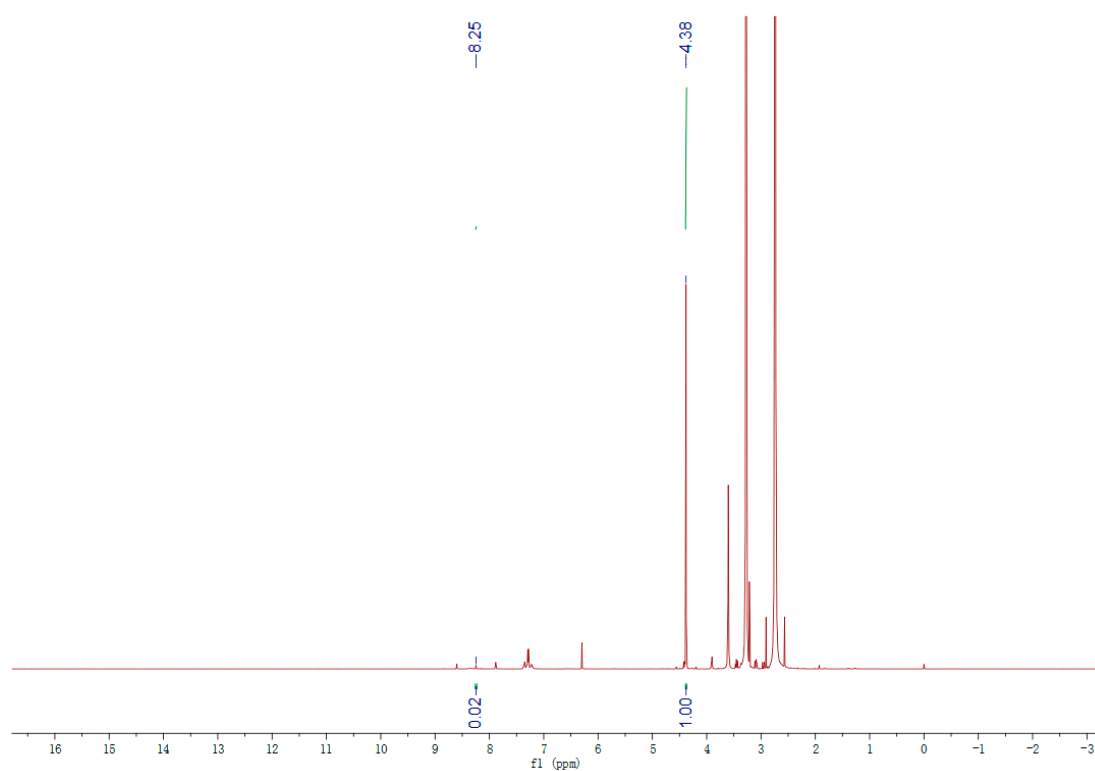
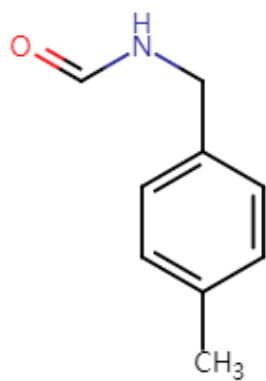


**Figure S5** NMR spectrum of reaction solution of 4a reacting with CO<sub>2</sub>/H<sub>2</sub> (CH<sub>3</sub>NO<sub>2</sub>: 0.0248 g).





5b

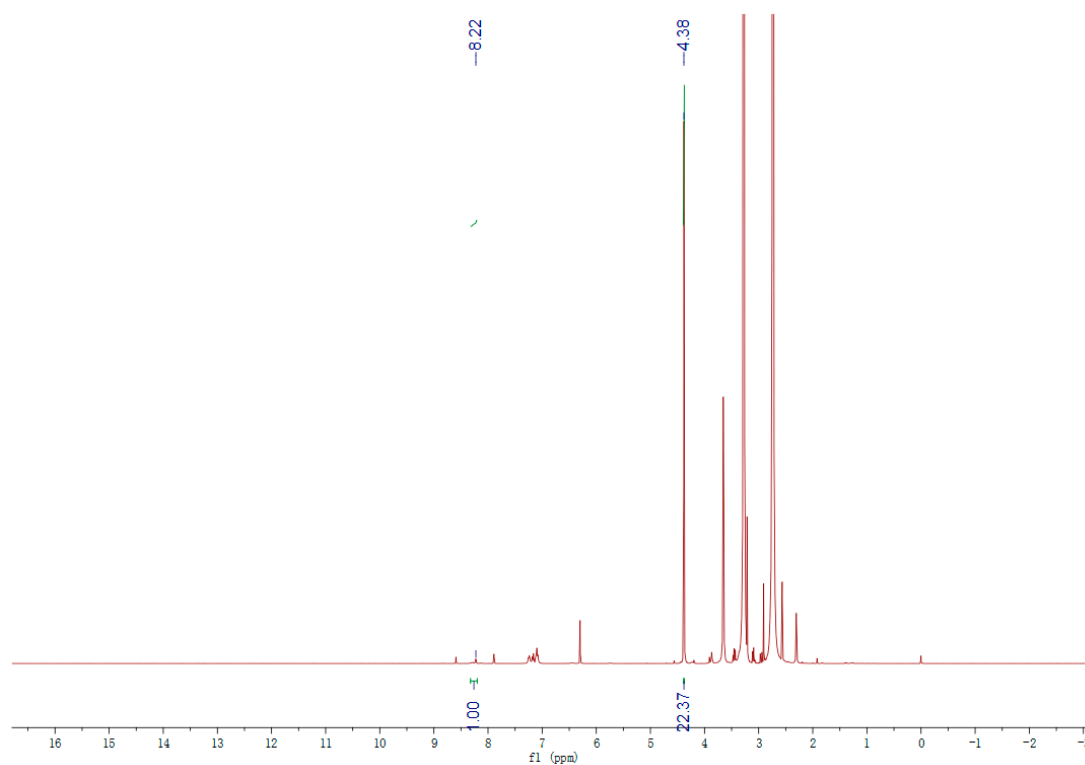
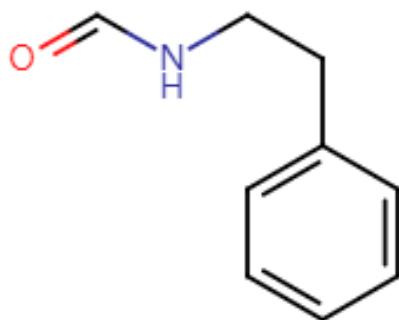


**Figure S6** NMR spectrum of reaction solution of 5a reacting with CO<sub>2</sub>/H<sub>2</sub> (CH<sub>3</sub>NO<sub>2</sub>: 0.0233 g).



6b

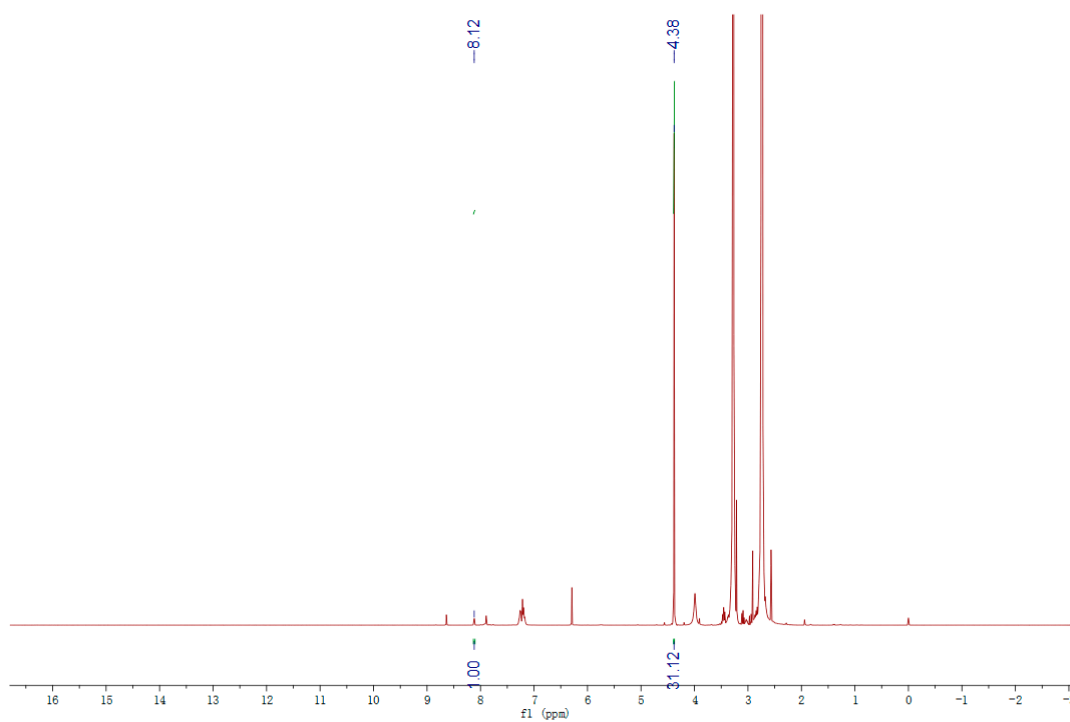
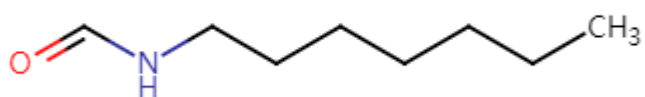


**Figure S7** NMR spectrum of reaction solution of 6a reacting with CO<sub>2</sub>/H<sub>2</sub> (CH<sub>3</sub>NO<sub>2</sub>: 0.0227g).



7b

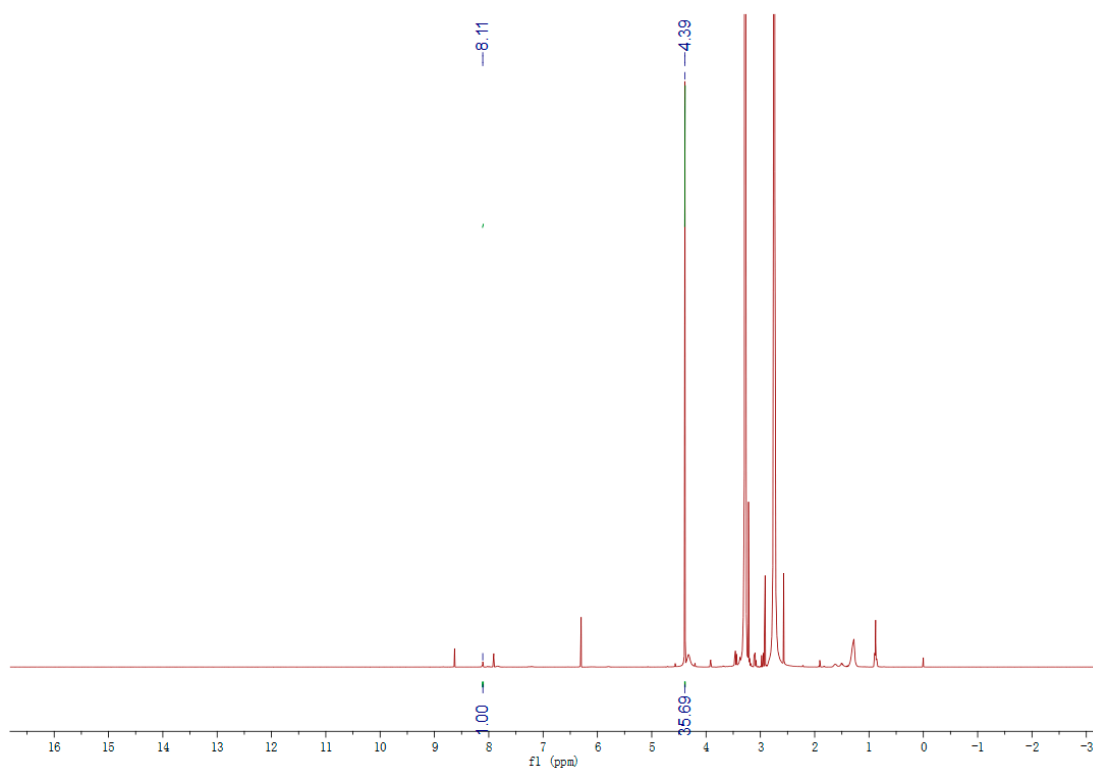
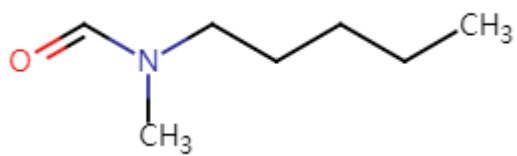


**Figure S8** NMR spectrum of reaction solution of 7a reacting with  $\text{CO}_2/\text{H}_2$  ( $\text{CH}_3\text{NO}_2$ : 0.0235 g).



8b

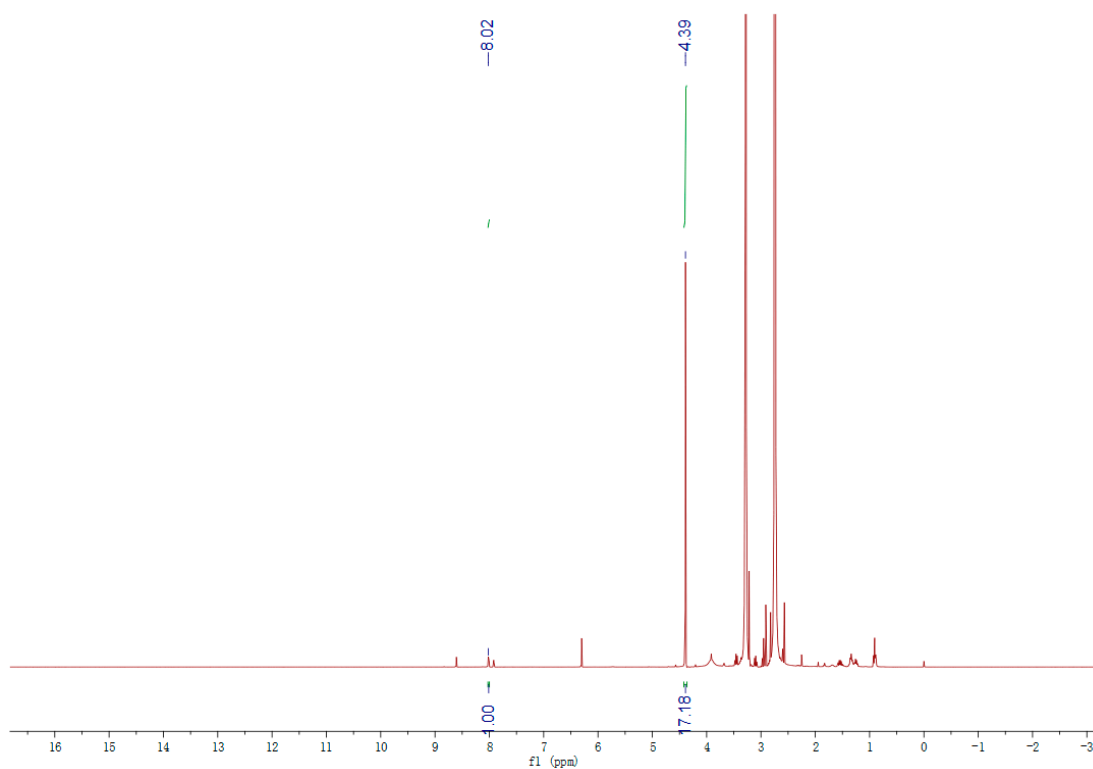
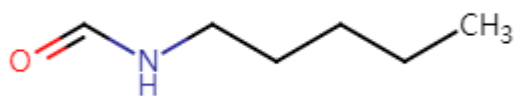


**Figure S9** NMR spectrum of reaction solution of 8a reacting with CO<sub>2</sub>/H<sub>2</sub> (CH<sub>3</sub>NO<sub>2</sub>: 0.0214 g).



9b

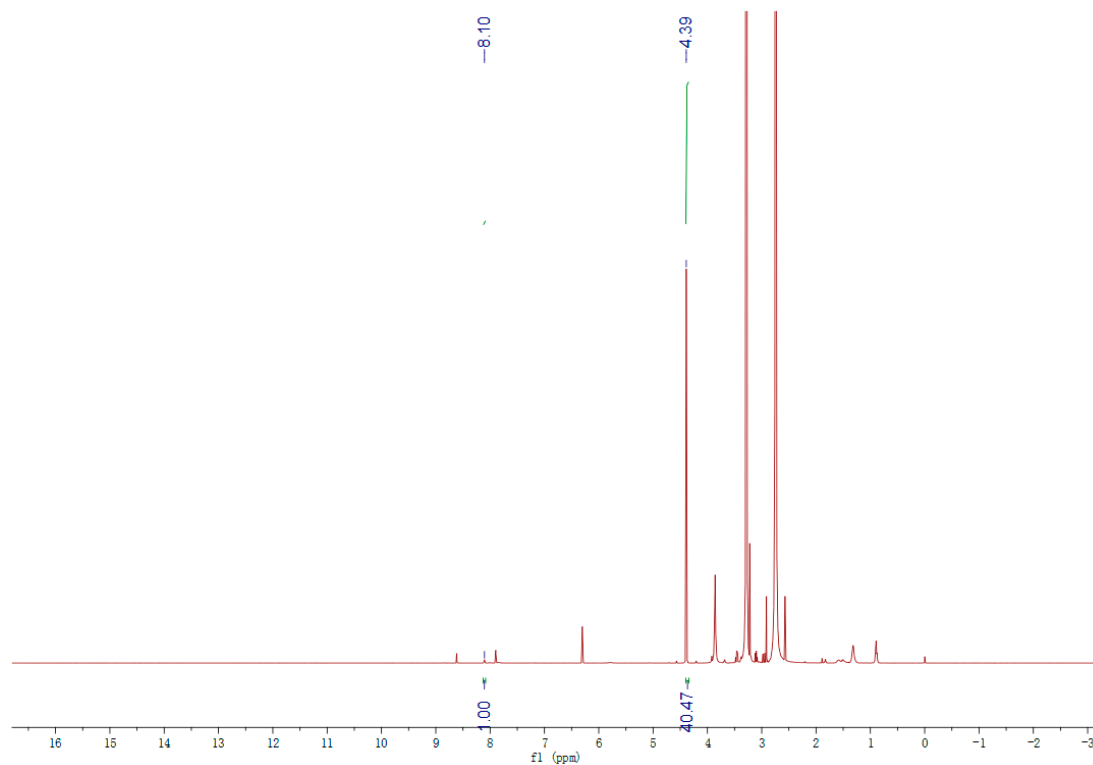


**Figure S10** NMR spectrum of reaction solution of 9a reacting with CO<sub>2</sub>/H<sub>2</sub> (CH<sub>3</sub>NO<sub>2</sub>: 0.0235 g).